Engineering supermode silicon/III–V hybrid waveguides for laser oscillation

Xiankai Sun* and Amnon Yariv

Department of Applied Physics, MC128-95, California Institute of Technology, Pasadena, California 91125, USA
**Corresponding author: xksun@caltech.edu*

Received January 3, 2008; accepted March 17, 2008;
posted April 1, 2008 (Doc. ID 91270); published May 14, 2008

We analyze a silicon/III–V hybrid semiconductor waveguide structure for laser oscillation. We show that, by optimally designing and controlling the resonant supermode behavior in such structures, the modal gain can be enhanced five times compared with that of the existing silicon evanescent laser, while maintaining efficient coupling to outside silicon waveguide circuits. © 2008 Optical Society of America

OCIS codes: 250.3140, 130.2790, 130.3120, 140.5960.

During the past two decades, there has been an ever-increasing pace of activity in the area of realizing laser emission from silicon (Si) [1–6]. Recently, we proposed a novel supermode Si/III–V hybrid waveguide system for laser oscillation, amplification, and modulation [7]. The structure is illustrated in Fig. 1. The hybrid device consists of two parallel waveguides in close proximity coupled to each other. The top waveguide is fabricated in a III–V compound semiconductor and supplies the gain, and the bottom is a waveguide fabricated in Si. The eigenmodes of this hybrid structure, the supermodes, can be controlled by suitable design of dimensions of the waveguides [7]. The supermode is thus designed such that, in the left region (main body) most of the modal energy is concentrated in the III–V waveguide so that the mode experiences maximal gain, while in the right region near the output facet, the width of the Si waveguide is widened adiabatically so that most of the mode transforms to the Si waveguide for coupling to other Si photonic circuits. The fundamental difference between this scheme and the reported evanescent lasers by Fang *et al.* [6] is the use of supermode coupling rather than evanescent coupling. This makes it possible to fundamentally break the trade-off between the gain available to an optical mode and the output coupling efficiency intrinsic to the hybrid evanescent lasers. Therefore we expect a laser designed with this principle to operate with higher efficiency and be far shorter.

In this paper, we address several issues in engineering the supermode hybrid Si/III–V waveguide structure for laser oscillation. By optimally designing the III–V wafer layer structure, the III–V waveguide width, the Si waveguide width, and the adiabatic taper, we will show that the modal gain in the supermode resonator can be improved by a factor of 5 compared with that in the reported evanescent lasers. Finally, we will discuss the tolerance of misalignment of the two waveguides during fabrication.

First we focus on the optimal layer structure of the III–V active wafer. In the evanescent laser design by Fang *et al.* [6], the quantum wells (QWs) needed to be as close to the Si waveguide as possible to have more of the mode field evanescently penetrating into the QW region. In our supermode scheme, the resonant supermode can have most of the energy concentrated in the III–V waveguide without reducing the distance between the QWs and the Si waveguide. Thus, we seek to engineer the wafer to make full use of the available gain from the QWs. Since all the epi-grown layers must be perfectly lattice matched to the InP substrate, we can, most simply and effectively, modify only the thicknesses of the separate confinement heterostructure (SCH) layer and n-layer of the wafer design in [6] to improve the modal confinement in the QWs. By choosing the thicknesses of the SCH layer and the n-layer to be 80 and 200 nm, respectively, we obtain a maximal confinement factor in the active region (QWs and barriers in between) Γ_{act} of 0.348 in the absence of a Si waveguide. This is ~30% larger than that of the wafer design presented in [6] calculated under the same condition.

Next we design the constituent waveguides of the hybrid structure. From the supermode theory [8], the eigenmodes of the coupled waveguides (supermodes) are linear combinations of those of the uncoupled waveguides. The modal field distributions and the phase velocities of the supermodes are determined by the phase mismatch parameter δ and the amplitude spatial overlap κ between the modes of the uncoupled waveguides. In a 2-D geometry, δ and κ are defined as

$$\delta = \frac{(\beta_b + M_b) - (\beta_a + M_a)}{2}, \tag{1}$$

$$\kappa = (\kappa_{ab}\kappa_{ba})^{1/2}, \tag{2}$$

where

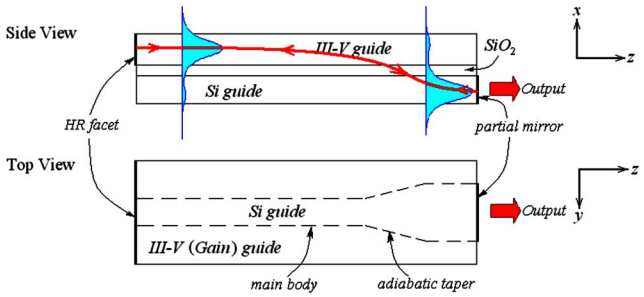

Fig. 1. (Color online) (Top) Side view of the proposed hybrid laser and the evolution of the lasing supermode inside the hybrid waveguide resonator. (Bottom) Adiabatic widening of the silicon waveguide causes the supermode power to transfer from the upper amplifying III–V section to the lower silicon waveguide.

$$\kappa_{ab} = \frac{\omega\varepsilon_0}{4}\iint_{\infty}[n_c^2(x,y) - n_b^2(x,y)]\xi^{(a)}(x,y)\xi^{(b)}(x,y)\mathrm{d}x\mathrm{d}y, \tag{3}$$

$$\kappa_{ba} = \frac{\omega\varepsilon_0}{4}\iint_{\infty}[n_c^2(x,y) - n_a^2(x,y)]\xi^{(a)}(x,y)\xi^{(b)}(x,y)\mathrm{d}x\mathrm{d}y. \tag{4}$$

In the above expressions, β_a and β_b are the propagation constants of the uncoupled waveguide modes. M_a and M_b are small corrections to the propagation constants β_a and β_b, respectively, due to the presence of the other waveguide. $\xi^{(a)}(x,y)$ and $\xi^{(b)}(x,y)$ are the power-normalized modal distributions of the uncoupled waveguides. $n_a(x,y)$, $n_b(x,y)$, and $n_c(x,y)$ are the refractive index profiles of the uncoupled waveguides a and b and the coupled waveguide system c, respectively. By adjusting $n_a(x,y)$, $n_b(x,y)$, and $n_c(x,y)$, we can control δ and κ and thus allocate the energy in each waveguide as desired.

The supermodes of the hybrid waveguides arise from the coupling between all the original modes of the III–V waveguide and the Si waveguide. However, we are interested in the two lowest-order supermodes, which result from the coupling between the fundamental modes of the III–V and the Si waveguides. For the simulation, we use the aforementioned optimal III–V wafer structure with a waveguide width of 3.30 μm. The effective index n_{eff} is 3.2588 at the target wavelength of 1.55 μm as calculated with a mode solver. Figures 2(a) and 2(b) show the refractive index profile and the fundamental mode of the III–V waveguide. To achieve the phase-matching condition ($\delta \to 0$), we use a Si-on-silica waveguide with height $H = 0.84$ μm and width $W = 0.65$ μm, which possesses a n_{eff} of 3.2529. Figures 2(c) and 2(d) show the refractive index profile and the fundamental mode of the Si waveguide. The composite hybrid structure consists of the III–V and Si waveguides separated by a 10 nm thick layer of silica, as shown in Fig. 2(e). The thin silica layer is considered to assist in a low-temperature wafer bonding process [9]. Figures 2(f) and 2(g) show the even and odd supermodes of the hybrid waveguides. We see that, for both even and odd modes, the energy is roughly evenly divided between the III–V and the Si waveguides, as predicted by the supermode theory.

We have shown that the even and odd supermodes coexist in the coupled waveguide system, though propagating at different phase velocities. In practice, we want a single mode to oscillate in such a structure. We can separate the two supermodes by adiabatically tapering the Si waveguide width to provide different amounts of feedback to different modes. Only the mode having stronger feedback will lase. Figure 3(a) shows the confinement factors in the active region Γ_{act} and in the Si waveguide Γ_{Si} for the lowest-order even supermode as a function of Si waveguide width W. Figure 3(b) shows the confinement factors in the whole III–V waveguide $\Gamma_{\mathrm{III-V}}$ and in the Si waveguide Γ_{Si} and the mismatch parameter δ as a function of Si waveguide width W. As expected, these three curves intersect at one point where the phase is perfectly matched

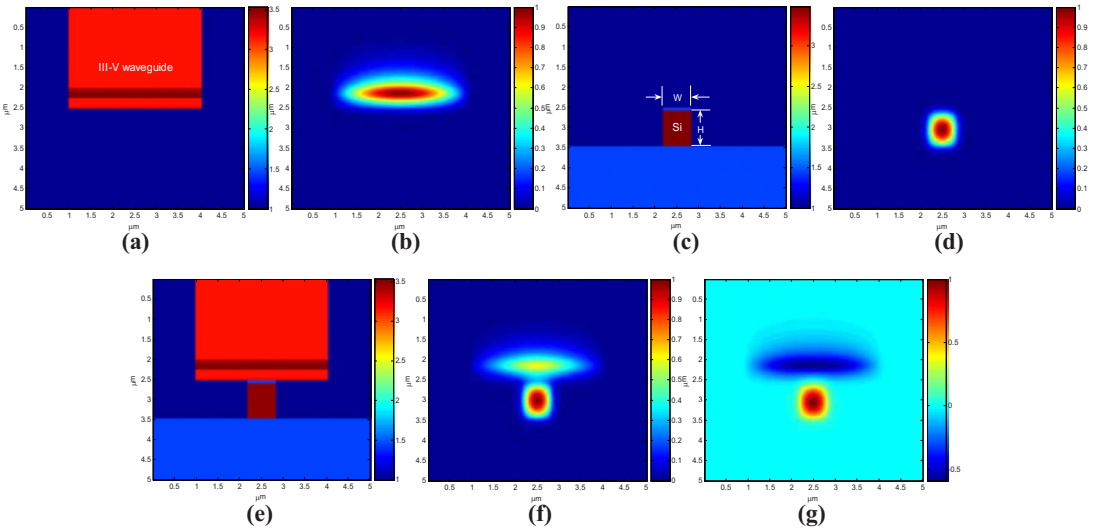

Fig. 2. (Color online) (a) Refractive index profile of the III–V waveguide. (b) Fundamental mode of the III–V waveguide. (c) Refractive index profile of the Si waveguide. (d) Fundamental mode of the Si waveguide. (e) Refractive index profile of the coupled system. (f) Even supermode of the coupled system (at the phase-matching point). (g) Odd supermode of the coupled system (at the phase-matching point).

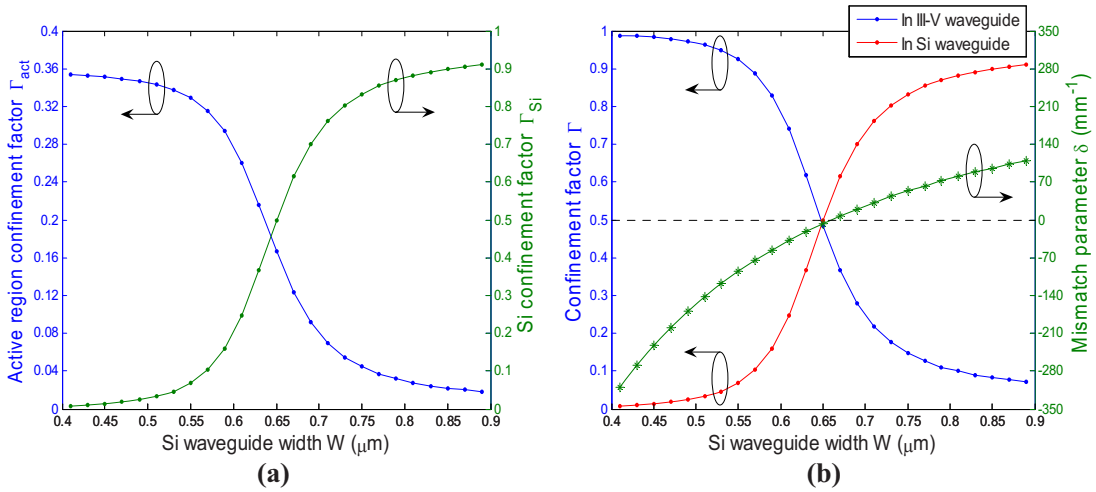

Fig. 3. (Color online) (a) Confinement factors in the active region (Γ_{act}) and in the Si waveguide (Γ_{Si}) as a function of Si waveguide width W. (b) Confinement factors in the III–V waveguide (Γ_{III-V}) and in the Si waveguide (Γ_{Si}) and the mismatch parameter δ as a function of Si waveguide width W.

($\delta \to 0$) and the energy is also evenly distributed in each waveguide.

In what follows we discuss the influence of the taper in our design. The taper is expected to adiabatically transform the mode at the main body, which has most of the energy confined to the III–V waveguide, to the mode near the end facet for output coupling. From Fig. 3, we choose to have at the main body a Si waveguide width of 0.51 μm and at the output facet a width of 0.89 μm, and we use an exponentially shaped taper as the transformer. Ideally we can have an output coupling efficiency of ~91%. Figure 4 displays the output power from the Si waveguide normalized by the input power into the taper region as a function of the taper length L. The results were computed using a beam propagation method. As we see, a taper with a length larger than 50 μm is sufficient to obtain the expected power conversion. We also notice that, for short taper lengths, the curve is strongly oscillatory with a half-periodicity of ~19 μm. Using tapers with lengths corresponding to those resonant coupling points [$L=(2n-1)19$ μm, $n=1,2,3$] may achieve even higher confinement in Si at the output facet than expected. This behavior, though beyond the adiabatic mode transforming scheme, can be understood by the supermode theory. Generally, in a system of two coupled waveguides, the propagation distance for power transferring from one waveguide to the other is $\pi/2\sqrt{\delta^2+\kappa^2}$ [8]. As the Si waveguide width varies from 0.51 to 0.89 μm, $|\delta|$ varies in the range of $0-142\ \mathrm{mm}^{-1}$ while κ stays roughly constant at $\sim 40\ \mathrm{mm}^{-1}$. The average distance for the power transfer estimated from the supermode theory agrees with the simulation results. In sum, if we use an exponentially shaped taper longer than 50 μm as well as the improved III–V wafer design, we can have at the main body $\Gamma_{act}=0.343$ and at the output facet $\Gamma_{Si}>0.855$. In the evanescent lasers, due to the trade-off between these two factors,

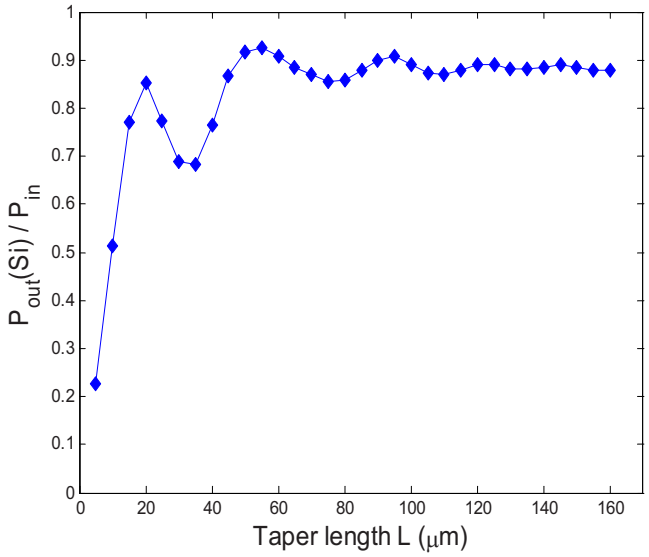

Fig. 4. (Color online) Normalized output power from the Si waveguide at the end of the taper as a function of the taper length L.

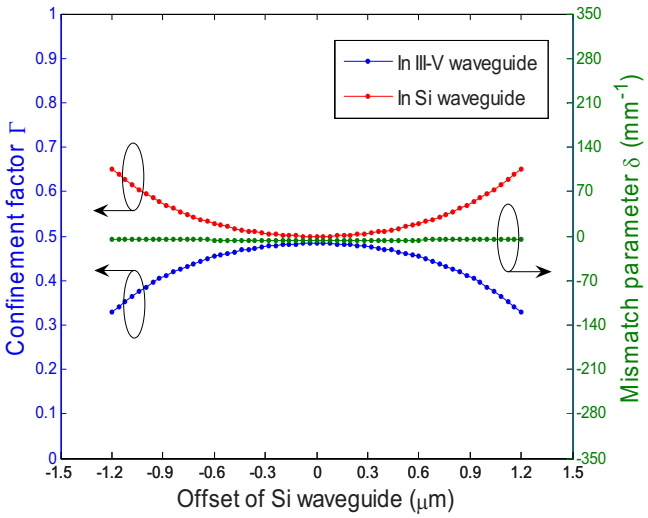

Fig. 5. (Color online) Confinement factors in the III–V waveguide (Γ_{III-V}) and in the Si waveguide (Γ_{Si}) and the mismatch parameter δ as a function of the offset of the Si waveguide from the center (at the phase-matching point).

a typical set of values are $\Gamma_{act}=0.067$ and $\Gamma_{Si}=0.757$. Thus, the average modal gain of the proposed supermode hybrid laser can be ~5 times higher than that of the evanescent laser, with also a higher output coupling efficiency. This implies that the supermode laser can be ~5 times shorter.

Finally, we discuss the important issue of tolerance of misalignment of the two waveguides. As mentioned before, the modal power distributions depend on the parameters δ and κ. If we consider the effect of only an offset of the Si waveguide from its designed center position, we do not expect a large change in δ and κ, since β_a and β_b do not change, and the changes in κ, M_a, and M_b are very small for the waveguide sizes considered. Figure 5 plots the calculated confinement factors in the III–V and the Si waveguides and also the mismatch parameter δ at the phase-matching point as a function of the offset of the Si waveguide. We find that even if the Si waveguide is moved to one edge of the III–V waveguide, $\pm 1.2\ \mu$m misaligned from the center, more than 30% of the energy still resides in the III–V waveguide.

In summary, we analyzed the supermode Si/III–V hybrid waveguide structure for laser oscillation. We discussed several issues in engineering this hybrid system by the supermode formalism. By optimally designing and controlling the lasing supermode behavior in the resonator, the modal gain can be increased by a factor of 5 compared with that in the Si evanescent lasers, while maintaining a high output coupling efficiency. An alignment accuracy of $\sim 1\ \mu$m can be tolerated. The supermode approach can also be extended to the design of other hybrid optical functional devices, such as an optical amplifier, phase or amplitude modulators, and coupled resonator waveguide systems.

ACKNOWLEDGMENTS

This work was supported by the Defense Advanced Research Projects Agency (DARPA). The authors thank J. Poon and L. Zhu for fruitful discussions and helpful comments.

REFERENCES

1. H. Z. Chen, A. Ghaffari, H. Wang, H. Morkoc, and A. Yariv, "Continuous-wave operation of extremely low-threshold GaAs/AlGaAs broad-area injection lasers on (100) Si substrates at room temperature," Opt. Lett. **12**, 812–813 (1987).
2. O. Boyraz and B. Jalali, "Demonstration of a silicon Raman laser," Opt. Express **12**, 5269–5273 (2004).
3. H. S. Rong, R. Jones, A. S. Liu, O. Cohen, D. Hak, A. Fang, and M. Paniccia, "A continuous-wave Raman silicon laser," Nature **433**, 725–728 (2005).
4. H. S. Rong, S. B. Xu, O. Cohen, O. Raday, M. Lee, V. Sih, and M. Paniccia, "A cascaded silicon Raman laser," Nat. Photonics **2**, 170–174 (2008).
5. S. G. Cloutier, P. A. Kossyrev, and J. Xu, "Optical gain and stimulated emission in periodic nanopatterned crystalline silicon," Nat. Mater. **4**, 887–891 (2005).
6. A. W. Fang, H. Park, O. Cohen, R. Jones, M. J. Paniccia, and J. E. Bowers, "Electrically pumped hybrid AlGaInAs–silicon evanescent laser," Opt. Express **14**, 9203–9210 (2006).
7. A. Yariv and X. K. Sun, "Supermode Si/III–V hybrid lasers, optical amplifiers and modulators: a proposal and analysis," Opt. Express **15**, 9147–9151 (2007).
8. A. Yariv, *Optical Electronics in Modern Communications*, 5th ed. (Oxford U. Press, 1997), pp. 526–531.
9. D. Pasquariello and K. Hjort, "Plasma-assisted InP-to-Si low temperature wafer bonding," IEEE J. Sel. Top. Quantum Electron. **8**, 118–131 (2002).